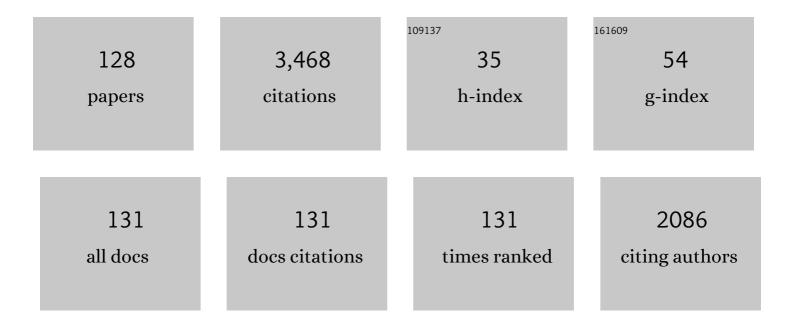
James H Churnside

List of Publications by Year in descending order

Source: https://exaly.com/author-pdf/7940493/publications.pdf Version: 2024-02-01



#	Article	IF	CITATIONS
1	Aperture averaging of optical scintillations in the turbulent atmosphere. Applied Optics, 1991, 30, 1982.	2.1	166
2	Marine debris collects within the North Pacific Subtropical Convergence Zone. Marine Pollution Bulletin, 2007, 54, 1207-1211.	2.3	149
3	Review of profiling oceanographic lidar. Optical Engineering, 2013, 53, 051405.	0.5	129
4	Log-normal Rician probability-density function of optical scintillations in the turbulent atmosphere. Journal of the Optical Society of America A: Optics and Image Science, and Vision, 1987, 4, 1923.	0.8	125
5	Scanning-laser glint measurements of sea-surface slope statistics. Applied Optics, 1997, 36, 4202.	2.1	119
6	Thin scattering layers observed by airborne lidar. ICES Journal of Marine Science, 2009, 66, 778-789.	1.2	108
7	Probability density of irradiance scintillations for strong path-integrated refractive turbulence. Journal of the Optical Society of America A: Optics and Image Science, and Vision, 1987, 4, 727.	0.8	99
8	Polarization lidar measurements of honey bees in flight for locating land mines. Optics Express, 2005, 13, 5853.	1.7	94
9	Airborne lidar for fisheries applications. Optical Engineering, 2001, 40, 406.	0.5	80
10	Going Beyond Standard Ocean Color Observations: Lidar and Polarimetry. Frontiers in Marine Science, 2019, 6, .	1.2	80
11	The Optical Properties of Equatorial Cirrus from Observations in the ARM Pilot Radiation Observation Experiment. Journals of the Atmospheric Sciences, 1998, 55, 1977-1996.	0.6	79
12	Wander of an optical beam in the turbulent atmosphere. Applied Optics, 1990, 29, 926.	2.1	78
13	Ocean subsurface studies with the CALIPSO spaceborne lidar. Journal of Geophysical Research: Oceans, 2014, 119, 4305-4317.	1.0	74
14	Laser Doppler velocimetry by modulating a CO_2 laser with backscattered light. Applied Optics, 1984, 23, 61.	2.1	66
15	Inner-scale effect on irradiance variance measured for weak-to-strong atmospheric scintillation. Journal of the Optical Society of America A: Optics and Image Science, and Vision, 1993, 10, 2354.	0.8	66
16	Temperature Profiling with Neural Network Inversion of Microwave Radiometer Data. Journal of Atmospheric and Oceanic Technology, 1994, 11, 105-109.	0.5	62
17	Polarization effects on oceanographic lidar. Optics Express, 2008, 16, 1196.	1.7	62
18	Thermal Footprints of Whales. Oceanography, 2009, 22, 206-209.	0.5	56

#	Article	IF	CITATIONS
19	GhostNet marine debris survey in the Gulf of Alaska – Satellite guidance and aircraft observations. Marine Pollution Bulletin, 2012, 65, 28-41.	2.3	54
20	Speckle from a rotating diffuse object. Journal of the Optical Society of America, 1982, 72, 1464.	1.2	53
21	Lidar observation of a strongly nonlinear internal wave train in the Gulf of Alaska. International Journal of Remote Sensing, 2005, 26, 167-177.	1.3	52
22	Airborne sensors for detecting large marine debris at sea. Marine Pollution Bulletin, 2012, 65, 63-68.	2.3	51
23	Oceanographic lidar profiles compared with estimates from in situ optical measurements. Applied Optics, 2013, 52, 786.	0.9	51
24	Experimental evaluation of log-normally modulated Rician and IK models of optical scintillation in the atmosphere. Journal of the Optical Society of America A: Optics and Image Science, and Vision, 1989, 6, 1760.	0.8	50
25	Lidar profiles of fish schools. Applied Optics, 1997, 36, 6011.	2.1	50
26	Infrared spectral radiance measurements in the tropical Pacific atmosphere. Journal of Geophysical Research, 1997, 102, 4353-4356.	3.3	50
27	Subsurface plankton layers in the Arctic Ocean. Geophysical Research Letters, 2015, 42, 4896-4902.	1.5	50
28	A comparison of lidar and echosounder measurements of fish schools in the Gulf of Mexico. ICES Journal of Marine Science, 2003, 60, 147-154.	1.2	43
29	Comparison of airborne lidar measurements with 420 kHz echo-sounder measurements of zooplankton. Applied Optics, 2005, 44, 5504.	2.1	43
30	Airborne lidar detection and characterization of internal waves in a shallow fjord. Journal of Applied Remote Sensing, 2012, 6, 063611.	0.6	42
31	Oceanographic lidar attenuation coefficients and signal fluctuations measured from a ship in the Southern California Bight. Applied Optics, 1998, 37, 3105.	2.1	40
32	Transient radiative transfer equation applied to oceanographic lidar. Applied Optics, 1999, 38, 889.	2.1	38
33	Lidar extinction-to-backscatter ratio of the ocean. Optics Express, 2014, 22, 18698.	1.7	38
34	Remote sensing of capelin and other biological features in the North Pacific using lidar and video technology. ICES Journal of Marine Science, 2002, 59, 1120-1130.	1.2	37
35	Comparison of airborne lidar with echosounders: a case study in the coastal Atlantic waters of southern Europe. ICES Journal of Marine Science, 2006, 63, 1736-1750.	1.2	37
36	Subsurface Ocean Signals from an Orbiting Polarization Lidar. Remote Sensing, 2013, 5, 3457-3475.	1.8	36

#	Article	IF	CITATIONS
37	Angle-of-arrival fluctuations of a reflected beam in atmospheric turbulence. Journal of the Optical Society of America A: Optics and Image Science, and Vision, 1987, 4, 1264.	0.8	35
38	Vertical distributions of blooming cyanobacteria populations in a freshwater lake from LIDAR observations. Remote Sensing of Environment, 2019, 225, 347-367.	4.6	35
39	Signal-to-noise in a backscatter-modulated Doppler velocimeter. Applied Optics, 1984, 23, 2097.	2.1	33
40	Inversion of oceanographic profiling lidars by a perturbation to a linear regression. Applied Optics, 2017, 56, 5228.	2.1	31
41	A Spectrum of Refractive Turbulence in the Turbulent Atmosphere. Journal of Modern Optics, 1990, 37, 13-16.	0.6	29
42	Ocean Backscatter Profiling Using High-Spectral-Resolution Lidar and a Perturbation Retrieval. Remote Sensing, 2018, 10, 2003.	1.8	29
43	Velocity measurement using laser speckle statistics. Applied Optics, 1981, 20, 3539.	2.1	28
44	LASER SAFETY THRESHOLDS FOR CETACEANS AND PINNIPEDS. Marine Mammal Science, 2000, 16, 186-200.	0.9	27
45	Lidar signature from bubbles in the sea. Optics Express, 2010, 18, 8294.	1.7	27
46	Epipelagic fish distributions in relation to thermal fronts in a coastal upwelling system using high-resolution remote-sensing techniques. ICES Journal of Marine Science, 2011, 68, 1865-1874.	1.2	27
47	Optical Backscattering Measured by Airborne Lidar and Underwater Glider. Remote Sensing, 2017, 9, 379.	1.8	25
48	Dual-polarization airborne lidar for freshwater fisheries management and research. Optical Engineering, 2017, 56, 031221.	0.5	23
49	Airborne lidar detection and mapping of invasive lake trout in Yellowstone Lake. Applied Optics, 2018, 57, 4111.	0.9	21
50	Aerial surveys of fish in estuaries: a case study in Chesapeake Bay. ICES Journal of Marine Science, 2011, 68, 239-244.	1.2	20
51	Surveying the distribution and abundance of flying fishes and other epipelagics in the northern Gulf of Mexico using airborne lidar. Bulletin of Marine Science, 2017, 93, 591-609.	0.4	20
52	Airborne Remote Sensing of a Biological Hot Spot in the Southeastern Bering Sea. Remote Sensing, 2011, 3, 621-637.	1.8	20
53	Second harmonic generation using partially coherent light. Optics Communications, 1984, 51, 207-212.	1.0	19
54	Lidar remote sensing of the aquatic environment: invited. Applied Optics, 2020, 59, C92.	0.9	19

#	Article	IF	CITATIONS
55	Signal current probability distribution for optical heterodyne receivers in the turbulent atmosphere 1: Theory. Applied Optics, 1978, 17, 2141.	2.1	18
56	Relationships between water attenuation coefficients derived from active and passive remote sensing: a case study from two coastal environments. Applied Optics, 2011, 50, 2990.	2.1	18
57	Airborne lidar imaging of salmon. Applied Optics, 2004, 43, 1416.	2.1	16
58	Statistics of irradiance scattered from a diffuse target containing multiple glints. Journal of the Optical Society of America, 1980, 70, 1084.	1.2	15
59	Measured Statistics of Laser Beam Scintillation in Strong Refractive Turbulence Relevant to Eye Safety. Health Physics, 1987, 53, 639-647.	0.3	15
60	Observational challenges of strong scintillations of irradiance. Journal of the Optical Society of America A: Optics and Image Science, and Vision, 1988, 5, 445.	0.8	15
61	Optical properties of several Pacific fishes. Applied Optics, 1991, 30, 2925.	2.1	14
62	Enhanced backscatter of a reflected beam in atmospheric turbulence. Applied Optics, 1993, 32, 2651.	2.1	14
63	Angle-of-arrival fluctuations of retroreflected light in the turbulent atmosphere. Journal of the Optical Society of America A: Optics and Image Science, and Vision, 1989, 6, 275.	0.8	13
64	Ground-Based Remote Sensor Observations during PROBE in the Tropical Western Pacific. Bulletin of the American Meteorological Society, 1999, 80, 257-270.	1.7	13
65	Stratification, plankton layers, and mixing measured by airborne lidar in the Chukchi and Beaufort seas. Deep-Sea Research Part II: Topical Studies in Oceanography, 2020, 177, 104742.	0.6	13
66	Fractal laser glints from the ocean surface. Journal of the Optical Society of America A: Optics and Image Science, and Vision, 1997, 14, 1144.	0.8	12
67	Altair unmanned aircraft system achieves demonstration goals. Eos, 2006, 87, 197.	0.1	12
68	Comparison of data-processing algorithms for the lidar detection of mackerel in the Norwegian Sea. ICES Journal of Marine Science, 2009, 66, 1023-1028.	1.2	12
69	Refractive turbulence profiling using synthetic aperture spatial filtering of scintillation. Applied Optics, 1987, 26, 1295.	2.1	11
70	Aperture size and bandwidth requirements for measuring strong scintillation in the atmosphere. Applied Optics, 1989, 28, 4126.	2.1	11
71	î"k Lidar sensing of surface waves in a wave tank. Applied Optics, 1993, 32, 339.	2.1	11
72	Lidar target-strength measurements on Northeast Atlantic mackerel (Scomber scombrus). ICES Journal of Marine Science, 2006, 63, 677-682.	1.2	11

#	Article	IF	CITATIONS
73	Spatial coherence between remotely sensed ocean color data and vertical distribution of lidar backscattering in coastal stratified waters. Remote Sensing of Environment, 2010, 114, 2584-2593.	4.6	11
74	Calibration of an airborne oceanographic lidar using ocean backscattering measurements from space. Optics Express, 2019, 27, A536.	1.7	11
75	Observations of downwelling infrared spectral radiance at Mauna Loa, Hawaii during the 1997-1998 ENSO event. Geophysical Research Letters, 1999, 26, 1727-1730.	1.5	10
76	Hollow aggregations of moon jellyfish (<i>Aurelia</i> spp.). Journal of Plankton Research, 2016, 38, 122-130.	0.8	10
77	Averaged threshold receiver for direct detection of optical communications through the lognormal atmospheric channel. Applied Optics, 1977, 16, 2669.	2.1	9
78	Enhanced variance of irradiance from target glint. Applied Optics, 1979, 18, 3211.	2.1	9
79	Heterodyne receivers for atmospheric optical communications. Applied Optics, 1980, 19, 582.	2.1	9
80	Zernike-polynomial expansion of turbulence-induced centroid anisoplanatism. Optics Letters, 1985, 10, 258.	1.7	9
81	Localized measurements of refractive turbulence using spatial filtering of scintillations. Applied Optics, 1988, 27, 2199.	2.1	9
82	Air temperature profile and air/sea temperature difference measurements by infrared and microwave scanning radiometers. Radio Science, 2003, 38, n/a-n/a.	0.8	9
83	Signal current probability distribution for optical heterodyne receivers in the turbulent atmosphere 2: Experiment. Applied Optics, 1978, 17, 2148.	2.1	8
84	Joint probability-density function of irradiance scintillations in the turbulent atmosphere. Journal of the Optical Society of America A: Optics and Image Science, and Vision, 1989, 6, 1931.	0.8	8
85	Statistical Properties of Estimates of the Moments of Laser Scintillation. Journal of Modern Optics, 1989, 36, 1645-1659.	0.6	8
86	Two-color correlation of atmospheric scintillation. Applied Optics, 1992, 31, 4285.	2.1	8
87	Lidar measurements of the diffuse attenuation coefficient in Yellowstone Lake. Applied Optics, 2020, 59, 3097.	0.9	8
88	Comparison of Infrared Atmospheric Brightness Temperatures Measured by a Fourier Transform Spectrometer and a Filter Radiometer. Journal of Atmospheric and Oceanic Technology, 1995, 12, 1124-1128.	0.5	7
89	Visual demonstration of three-scale sea-surface roughness under light wind conditions. IEEE Transactions on Geoscience and Remote Sensing, 2005, 43, 1751-1762.	2.7	7
90	Power spectrum and fractal dimension of laser backscattering from the ocean. Journal of the Optical Society of America A: Optics and Image Science, and Vision, 2006, 23, 2829.	0.8	7

#	Article	IF	CITATIONS
91	Speckle correlation measurements using clipped intensity signals. Applied Optics, 1985, 24, 2488.	2.1	6
92	Effects of underwater sound and surface ripples on scattered laser light. Acoustical Physics, 2008, 54, 204-209.	0.2	6
93	Ocean Color Inferred from Radiometers on Low-Flying Aircraft. Sensors, 2008, 8, 860-876.	2.1	6
94	Ocean color patterns help to predict depth of optical layers in stratified coastal waters. Journal of Applied Remote Sensing, 2011, 5, 053548.	0.6	6
95	Scanning infrared radiometer for measuring the air–sea temperature difference. Applied Optics, 2001, 40, 4807.	2.1	5
96	LIDAR detection of plankton in the ocean. , 2007, , .		5
97	Bio-optical model to describe remote sensing signals from a stratified ocean. Journal of Applied Remote Sensing, 2015, 9, 095989.	0.6	5
98	Airborne Lidar Observations of a Spring Phytoplankton Bloom in the Western Arctic Ocean. Remote Sensing, 2021, 13, 2512.	1.8	5
99	Refractive turbulence profiling using stellar scintillation and radar wind profiles. Applied Optics, 1988, 27, 4884.	2.1	4
100	Infrared spectrometer for ground-based profiling of atmospheric temperature and humidity. , 1991, 1540, 681.		4
101	Image Jitter, Blur, and Scintillation Regarding the Retinal Hazards of Lasers. Health Physics, 1994, 66, 159-162.	0.3	4
102	Optical remote sensing of sound in the ocean. Journal of Applied Remote Sensing, 2015, 9, 096038.	0.6	4
103	Effect of penetration depth and swell-generated tilt on delta-k lidar performance. Applied Optics, 1994, 33, 2363.	2.1	3
104	Determination of ocean wave spectra from images of backscattered incoherent light. Applied Optics, 1995, 34, 962.	2.1	3
105	Airborne lidar detection of an underwater thermal vent. Journal of Applied Remote Sensing, 2017, 11, 1.	0.6	3
106	Partial tracking optical heterodyne receiver arrays. Journal of the Optical Society of America, 1978, 68, 1672.	1.2	2
107	Remote sensing of wind velocity and strength of refractive turbulence using a two-spatial-filter receiver. Applied Optics, 1994, 33, 5859.	2.1	2
108	<title>Can we see fish from an airplane?</title> . , 1999, , .		2

#	Article	IF	CITATIONS
109	Lidar as a tool for fisheries management. , 2011, , .		2
110	Applying Gaussian Mixture Models to Detect Fish from Airborne LiDAR Measurements. , 2021, , .		2
111	Combining Techniques for Remotely Assessing Pelagic Nekton: Getting the Whole Picture. , 2009, , 345-356.		2
112	Surveying the distribution and abundance of flying fishes and other epipelagics in the northern Gulf of Mexico using airborne lidar. Bulletin of Marine Science, 2016, , .	0.4	2
113	Review of profiling oceanographic lidar (erratum). Optical Engineering, 2017, 56, 079802.	0.5	2
114	Joint signal current probability distribution for optical heterodyne receiver arrays in the turbulent atmosphere. Applied Optics, 1979, 18, 2315.	2.1	1
115	Laser-glint techniques for sensing sea-surface roughness. , 1997, , .		1
116	<title>Infrared laser-glint sensor for measuring fractal sea-surface roughness</title> ., 1998, , .		1
117	Polarization lidar measurements of honeybees for locating buried landmines. , 2005, , .		1
118	Biological thin layers: history, ecological significance and consequences to oceanographic sensing systems. Proceedings of SPIE, 2012, , .	0.8	1
119	Effect of surface roughness on lidar overlap function. Proceedings of SPIE, 2013, , .	0.8	1
120	Airborne lidar estimates of photosynthesis profiles. , 2016, , .		1
121	Optical communications through a dispersive medium: a performance bound for photocounting. Applied Optics, 1981, 20, 573.	2.1	Ο
122	Possibilities of using IR spectrometer data for sizing cirrus cloud particles. , 1993, 1934, 381.		0
123	<title>Calculation of signals for oceanographic lidar</title> ., 1998, 3382, 134.		О
124	Airborne lidar sensing of internal waves in a shallow fjord. , 2012, , .		0
125	Ecosystem studies using profiling polarization LiDAR. , 2014, , .		0
126	Optical remote sensing of sound in the ocean. Proceedings of SPIE, 2014, , .	0.8	0

#	ARTICLE	IF	CITATIONS
127	Bio-optical model of remote sensing signals in a stratified ocean. , 2015, , .		0
128	Measurements of the attenuation coefficient of a lidar in the Southern California Bight. Proceedings of SPIE, 1997, , .	0.8	0